Design of adhesively bonded timber-concrete composites: Bondline properties

Philippe Grönquist, Institute of Construction Materials & Materials Testing Institute, University of Stuttgart, Germany

Katharina Müller, Lignolution GmbH, Zurich, Switzerland

Simon Mönch, Institute of Structural Design, University of Stuttgart, Germany

Andrea Frangi, Institute of Structural Engineering, ETH Zurich, Switzerland

1 Introduction

1.1 Background and motivation

Adhesive connections for timber-concrete composites (TCC) are of increasing popularity. Recent examples include, amongst others, studies by *Tannert* et al. (2020), *Frohnmüller* et al. (2021), *Kästner* & *Rautenstrauch* (2021), *Grönquist* et al. (2022), *Arendt* et al. (2022), *Frohnmüller* et al. (2023), and *Śliwa-Wieczorek* et al. (2023), where different possible execution types of adhesive bonding processes have successfully been applied. With this ongoing trend of intensive development in timber engineering research as well as in adhesive technology, the relevance and use in practice of adhesively bonded timber-concrete composite constructions (ATCC) is believed to substantially increase in the near future.

Up to the year 2021, no specific design guidelines were available for TCC elements in general. Mainly, annex B of EN 1995-1-1 (2004) provided the γ-method for the stress calculation of beams that are joined with mechanical fasteners characterized by a certain slip modulus *K*. The timber section could then be designed according to EN 1995-1-1 (2004), and the concrete section according to EN 1992-1-1 (2004). Out of necessity to address TCC-specific design aspects, e.g. long-term effects, a technical specification, CEN/TS 19103 (2021), was made available in 2021, based on a state of the art report by A. Dias et al. (2018). However, the technical specification is limited to the current practice-relevant connection methods for TCC, i.e. different metallic fastener and notch types. It is yet unclear how the adhesively bonded connection type shall be considered, as it is excluded from CEN/TS 19103 (2021).

Regardless of whether flat or ribbed ATTC slabs are to be designed, there are different options regarding the adhesive with respect to (1) process (wet or dry), (2) bondline arrangement (a continuous or multiple discontinuous bondlines), or (3) type of adhesive (rigid or flexible). Table 1 provides an overview. These different execution types inherently result in different bondline and composite properties that shall be taken into account in

the design procedure. However, no consensus on specific suggestions or rules, respecting the different execution types, yet exist.

Table 1. Overview of different possible ATCC execution types and recent literature examples from years 2020-2023.

Execution type	Definition	Recent examples
Dry process	Prefabricated concrete element bonded to timber	*Frohnmüller* et al., 2021; *Fu* et al., 2022; *Frohnmüller* et al., 2023
Wet process	(Wet) In-situ concrete poured on (wet) adhesive applied on timber surface	*Tannert* et al., 2020; *Grönquist* et al., 2022; *Füchslin* et al., 2023; *Arendt* et al., 2022; *Bajzecerová* et al., 2022
Continuous bondline	Adhesive applied to cover the whole available interfacial area between timber and concrete	*Tannert* et al., 2020; *Grönquist* et al., 2022; *Arendt* et al., 2022; *Bajzecerová* et al., 2022; *Fu* et al., 2022
Discontinuous bondlines	Adhesive applied locally, to partly cover the available interfacial area, e.g. as strips longitudinal or perpendicular to the span direction	*Frohnmüller* et al. (2021, 2023)
Rigid adhesive / rigid interlayer	High elastic modulus adhesives, e.g. epoxy-based adhesives with $E_{adh} \approx 2 - 7$ GPa	*Tannert* et al. (2020), *Arendt* et al. (2022), *Grönquist* et al. (2022), *Frohnmüller* et al. (2021), *Bajzecerová* et al. (2022), *Fu* et al. (2022), and *Frohnmüller* et al. (2023)
Flexible adhesive / flexible interlayer	Low elastic modulus adhesives, e.g. polyurethane-based adhesives with $E_{adh} \approx 0.01 - 1$ GPa	Hackspiel (2020), *Fu* et al. (2022), and *Śliwa-Wieczorek* et al. (2023)

1.2 Objectives and scope

This paper shall present some preliminary design consideration for ATCC elements. Hereby, the focus will be laid on bondline connection properties and how they may be influenced by the execution type (Section 2), and on possible ULS and SLS design (Section 3). The presented insight shall be based on current available literature and experience, as well as on exemplary parametric studies. The objective of this study is to lead to a discussion about ATCC-specific design aspects that could be worked-out in the future, and with which CEN/TS 19103 (2021) could potentially be extended. In this paper, a general knowledge from the reader on the design of TCC elements according to CEN/TS 19103 (2021) is presupposed. The study focuses on and is limited to the possibilities of simplified design methods (i.e. using the γ-method), and excludes more complex analysis possibilities (e.g. a Finite Element based investigation and design, such as suggested in *Töpler* et al. (2023)).

2 Adhesive bondline connection properties

2.1 Determination of bondline strength

Bondline strength can typically be determined using multiple testing procedures. Examples include e.g. direct shear tests (block-shear or pushout tests), or bending tests where the bondline is calibrated to fail. In both cases, differently sized specimens (scales) are possible, and every testing procedure possesses specific advantages and disadvantages. In general, it has to be considered that experimentally tested adhesive bondline shear strengths will be dependent on specimen size, on the time at which the test is conducted with respect to the hardening state of the concrete (shrinkage and creep influences on stress state at bondline), as well as on the testing conditions (e.g. time to failure, climatic conditions). These influences challenge the standardization of possible testing procedures for ATCC bondlines. As an example, for a wet process execution type and tests conducted 28 days after casting of the concrete, symmetric double-shear pushout tests in *Füchslin* et al. (2023) show strongly size-dependent results. The results were yet different when the same adhesive and bondline configuration is tested on full-scale bending specimens (*Grönquist* et al. (2022)). The latter testing method is the most intensive in terms of preparation and cost, but a-priori the only one to truly reflect realistic execution conditions and bondline sizes (e.g. surface area and thickness) for reliable parameter determination for ultimate limit state (ULS) design. Therefore, until further investigations and insight on possibly less conservative methods (e.g. using size factors) are available for each possible execution type in particular, it can be recommended that the shear strength of ATCC adhesive bondlines be determined with full-scale bending tests. Hereby, characteristic values can be derived according to EN 14358 (2016).

2.2 Determination of bondline stiffness

2.2.1 Rigid bondlines

Typically, for the ULS and serviceability limit state (SLS) design of adhesively bonded composite elements, basic mechanic principles, i.e. Steiner's theorem, can be used. In fact, most adhesive bondlines can be considered as rigid bonds. If the γ-method of annex B of EN 1995-1-1 (2004) would be used for ATCC elements, this would correspond to a value of $\gamma = 1$. Therefore, the need to determine and use a slip modulus or connection stiffness K_{ser}[1] for adhesive bondlines can be relativized. For metallic fasteners and notches, annex C of CEN/TS 19103 (2021) provides a testing procedure in the form of pushout tests in order to determine K_{ser}, and therewith, depending on the connector design and arrangement, the composite factor γ can be calculated. For ATCC, results of such pushout tests are provided e.g. in *Füchslin* et al. (2023) or in *Tannert* et al. (2020),

[1] Note: For connection systems with a high stiffness and a distinct linear elastic phase, e.g. notches, glued-in shear connectors, or adhesive bondlines, $K = K_{ser} = K_u$ can be used (see A. M. P. G. Dias (2005) and *Müller* (2020)), and will herein be referred to as K_{ser}.

where values for K_{ser} have been derived using symmetric double-shear pushout tests. These studies could in fact report, on average, high values for K_{ser} (> 1′000 kN/mm), such that for most practical cases $\gamma \approx 1$. However, in general, it can be suggested that a bondline slip modulus $K_{ser,adh}$ [kN/mm] is experimentally determined and used in design as follows:

$$K_{ser,adh} = K'_{ser,adh} \cdot b_{adh} \cdot L_{adh}, \tag{1}$$

where $K'_{ser,adh}$ [kN/(mm·mm'·mm")] is an experimentally determined bondline slip modulus normalized by the width [mm'] and length [mm"] of the bondline of the tested specimens, and b_{adh} [mm] is the width and L_{adh} [mm] is the length of the adhesive bondline in the current design situation. The resulting composite factor γ, when taking the timber section as reference (subscript *t* for timber, *c* for concrete), will then be:

$$\gamma = \left(1 + \frac{\pi^2 E_c A_c s_{eff}}{L_{ref}^2 K_{ser,adh}}\right)^{-1}, \tag{2}$$

where E_c is the elastic modulus of concrete, A_c is the cross-sectional area of concrete, s_{eff} is an effective distance of connections (bondlines), and L_{ref} is the span. In case of a continuous bondline over the whole length of the ATCC element, s_{eff} = 1 [mm]. In the case of discontinuous bondlines over the length, it is recommended to calculate s_{eff} e.g. as suggested in the case of micro-notches in *Müller* (2020), or as in *Michelfelder* (2006). In the case of discontinuous bondlines over the width, b_{adh} can be considered according to Eq. 1.

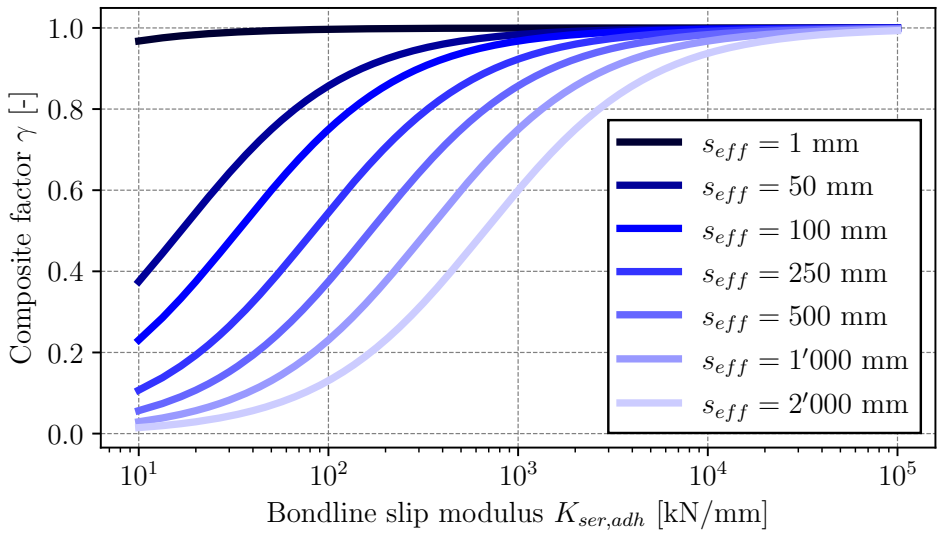

Figure 1. γ-values as a function of different values for $K_{ser,adh}$ and in dependence of distances s_{eff} in order to consider discontinuous bondlines. The example situation considers the timber section as reference, a span of L = 5 m, a concrete cross-section strip of h x b = 80 mm x 320 mm, and a concrete of class C30/37). See Fig. A.1 for a translation from γ to $EI_{ef}/EI_{\gamma=1}$.

With the exemplary parametric study presented in Fig. 1, it can be seen that even for rigid adhesives, i.e. where $K_{ser,adh}$ > 1′000 kN/mm, lower composite factors[2] result with discontinuous bondlines, in dependence of s_{eff}. Hereby, the influence of s_{eff} increases with decreasing $K_{ser,adh}$. However, it can be seen that for most cases where s_{eff} = 1 [mm], i.e. for continuous bondlines, the composite factor is effectively $\gamma \approx 1$, except for very low values of $K_{ser,adh}$ < 10 kN/mm. Accordingly, it can be said that in case of rigid adhesives and continuous bondlines, the determination of $K_{ser,adh}$ appears obsolete. However, this is not the case if the bondline is discontinuous, as here, a large influence of $K_{ser,adh}$ can be observed, and generally, $\gamma < 1$.

2.2.2 Flexible bondlines

In case the bondline or interlayer is to be considered flexible, i.e. if (1) it follows the definition from Table 1, or (2) it possesses a higher E-modulus but the adhesive bondline or interlayer is to be considered thick, the composite factor can presumably, and as an alternative to Eq. 2, be calculated in analogy to cross-laminated timber (transverse layers with rolling shear moduli) as follows:

$$\gamma = \left(1 + \frac{\pi^2 E_c h_c h_{adh}}{L_{ref}^2 G_{adh}}\right)^{-1}, \tag{3}$$

where G_{adh} [N/mm^2] is the shear modulus of the adhesive, h_{adh} is the thickness of the adhesive layer, and h_c is the height of the concrete. For isotropic adhesives, G_{adh} may be calculated as follows:

$$G_{adh} = \frac{E_{adh}}{2(1 + \nu_{adh})}, \tag{4}$$

where E_{adh} and ν_{adh} are the elastic modulus and the Poisson ratio of the adhesive. Furthermore, from Eq. 2, Eq. 3, and Eq. 4 it follows that:

$$K_{ser,adh} = \frac{G_{adh} b_{adh} s_{eff}}{h_{adh}} = \frac{E_{adh} b_{adh} s_{eff}}{2(1 + \nu_{adh}) h_{adh}}. \tag{5}$$

In Fig. 2, an exemplary parametric study is shown where $K_{ser,adh}$ and γ are investigated in dependence of the adhesive elastic modulus E_{adh}, and for different interlayer heights or adhesive thicknesses h_{adh}. It can be seen that the parameters E_{adh} and h_{adh} have a large influence on $K_{ser,adh}$ and γ. The latter is strongly affected in particular for adhesives where E_{adh} < 10 GPa, i.e. for most polyurethanes and epoxies, and where h_{adh} > 1 mm. However, the bondline could be considered to be fully rigid for E_{adh} > 10 GPa.

[2]Note: In the parametric studies (i.e. Fig. 1,Fig. 2, and Fig. 4), the timber section is taken as reference for the calculation of the composite factor γ. Fig. A.1 of the Appendix provides a translation from γ to true composite efficiency $EI_{ef}/EI_{\gamma=1}$ and a drawing of the example situation.

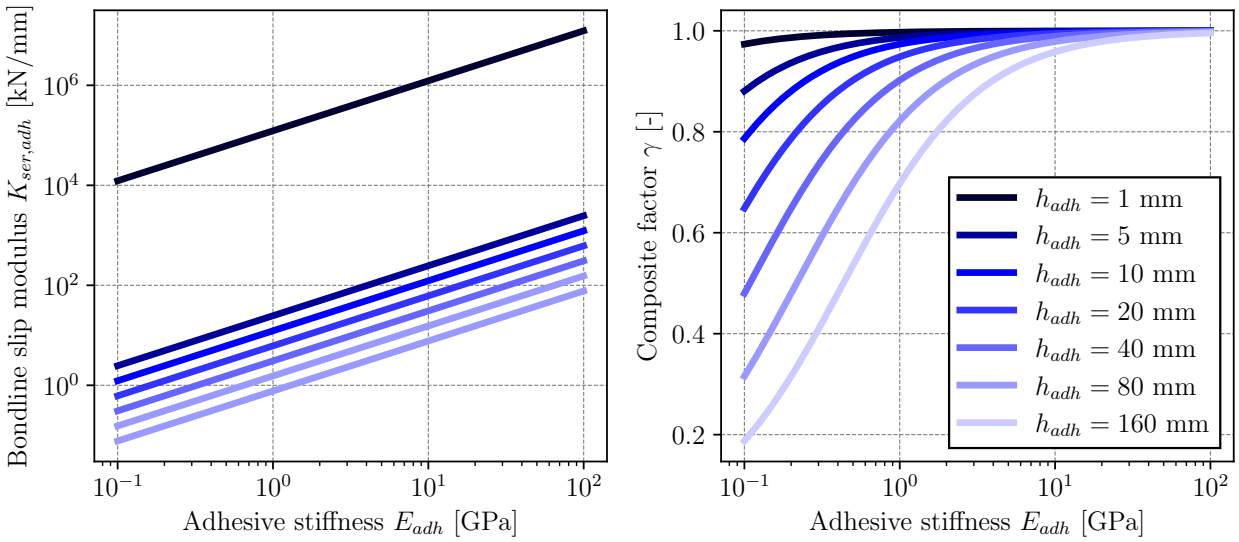

Figure 2. ***Left****: Bondline slip modulus $K_{ser,adh}$ as a function of different values for E_{adh} and in dependence of interlayer or bondline height h_{adh}.* ***Right****: γ-values as a function of different values for E_{adh} and in dependence of interlayer or bondline height h_{adh}. The example situation considers ν_{adh} = 0.3, a continuous bondline (s_{eff} = 1 mm), the timber section as reference, a span of L = 5 m, a concrete cross-section strip of h x b = 80 mm x 320 mm, and a concrete of class C30/37). See Fig. A.1 for a translation from γ to $EI_{ef}/EI_{\gamma=1}$.*

2.2.3 *Consideration of shear deformations in timber and concrete*

An important aspect regarding the transferability of experimentally determined stiffness values K_{ser} to composite factor values γ is the consideration of shear deformations. Shear deformations are normally neglected in the determination of the internal forces, except in the shear-analogy-method according to *Kreuzinger* (2000), or in DIN EN 1995-1-1/NA (2013). A study on the transferability of experimentally determined values of K_{ser} for TCC connectors with high stiffness values (notches) on pushout tests to similar experiments on TCC beams is given in *Schänzlin* & *Mönch* (2017). The study showed that the deformation of the beam can be slightly underestimated if the parameters obtained from pushout tests are used without considering the shear deformations. The latter can be considered by using

$$K_{eff} = \left(\frac{1}{K_{ser,adh}} + \frac{h_t}{2G_t b_t} + \frac{h_c}{2G_c b_c} \right)^{-1} \tag{6}$$

where K_{eff} [N/mm/mm] is the effective bondline slip modulus to be used for design in a slab or beam out-of-plane bending situation and under consideration of shear deformations in timber and concrete, per mm width. G_t [N/mm^2] and G_c [N/mm^2] are the sehar moduli of the timber and of the concrete, h_t [mm] and h_c [mm], and b_t [mm] and b_c [mm], are the height and the width of the timber and of the concrete, respectively. A parametric study on the influence of $K_{ser,adh}$ and G_t on K_{eff}, and of K_{eff} on γ is given in Fig. 3.

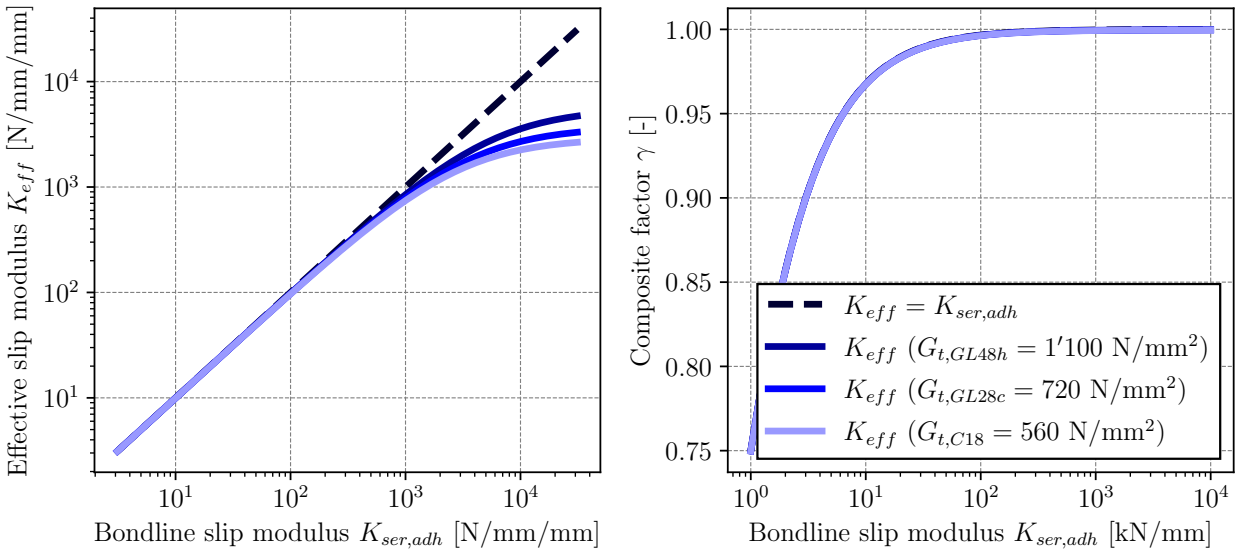

Figure 3. ***Left****: K_{eff}-values as a function of $K_{ser,adh}$ for different timber shear moduli G_t (GL48h, GL28c, and C18), and concrete shear modulus G_c (for C30/37 only), according to Eq. 6.* ***Right****: γ-values va. $K_{ser,adh}$ and as a function of K_{eff}. The example situation considers the timber section as reference, a span of L = 5 m, a concrete cross-section strip of h x b = 80 mm x 320 mm, and a concrete of class C30/37). See Fig. A.1 for a translation from γ to $EI_{ef}/EI_{\gamma=1}$.*

From Fig. 3 it can be seen that shear deformations in timber and concrete do not appear to influence γ. Even though, for $K_{ser,adh}$ > 1′000 N/mm/mm, the K_{eff} values seem to become relevant, they do not affect γ-values due to the fact that $\gamma \approx 1$ for $K_{ser,adh}$ > 1′000 kN/mm. Although further situations need be investigated, this is valid for the considered example situation. Furthermore, recalculations by *Grönquist* et al. (2022) on ATCC beam tests (experimental determination of EI_{ef}) using the γ-method showed that $\gamma \approx 1$. In such cases, it seems reasonable to neglect possible shear deformation effects.

2.3 Long-term reduction of connection stiffness for ULS and SLS design at $t \neq 0$

Comparing adhesive bonds with metallic fasteners or notches, it can be observed that there is no consistent reduction of K_{ser} (or K_u) by using the proposed reduction by the factor $(1 + \psi_{conn} k'_{def})$, as:

$$K_{ser,fin} = \frac{K_{ser}}{1 + \psi_{conn} k'_{def}}, \tag{7}$$

as suggested in CEN/TS 19103 (2021) for the time states t = 3 – 7 years and $t = \infty$ (considered with the factor ψ_{conn}). For metallic fasteners or notches, the reduction of the resulting γ-factor could be quite pronounced, while for an adhesive connection, there can be no reduction at all for values of $K_{ser,adh}$ > 100 kN/mm, as is exemplary illustrated in Fig. 4. In this exemplary parametric study, the effect of different possible adhesive creep factors ϕ_{adh} are investigated with respect to the resulting composite factor γ in

state $t = \infty$ (i.e. $\psi_{conn} = 1$). In fact, most adhesives, e.g. epoxy based adhesive possess a notorious visco-elastic creep behavior, where creep factors of $\phi_{adh} > 4$ are possible (depending on adhesive formulation). However, it can be seen that for bondlines with $K_{ser,adh} > 100$ kN/mm, the adhesive creep behavior has a negligible influence, and that $\gamma_{t=\infty} \approx 1$ can be safely assumed. For cases, where $K_{ser,adh} < 100$ kN/mm, it can be suggested that the adhesive creep factor ϕ_{adh} be experimentally determined, or that the suggested factor k'_{def} (red line in Fig. 4) be used. Next to simplified creep factors, adhesive creep compliance can experimentally be determined by suitable approaches, e.g. as done in Binder et al. (2023). This can include, in particular, fitting of linear visco-elastic creep parameters to experimental data in conjunction with the use of a suitable rheological model.

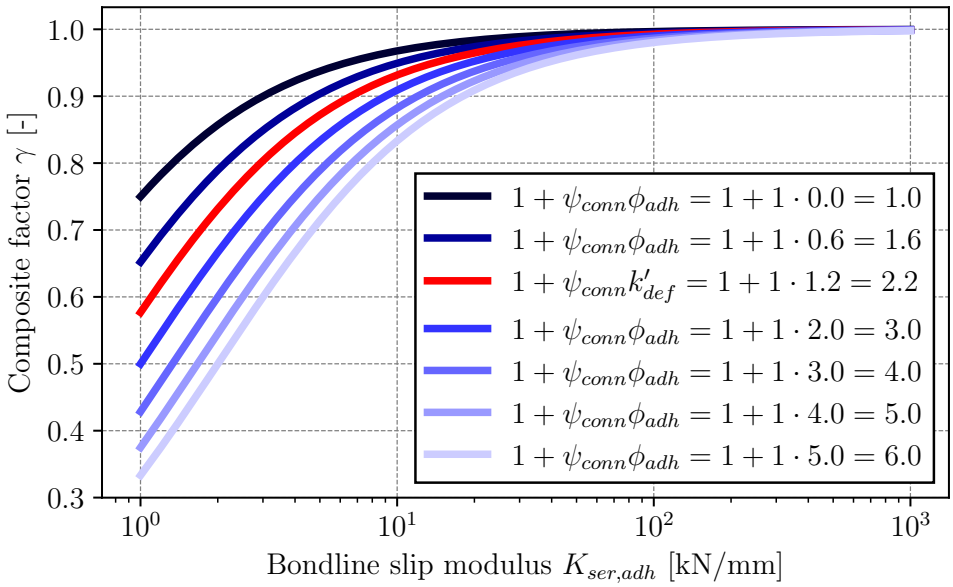

Figure 4. Obtained γ-values using $K_{ser,adh}$ (black curve) and $K_{ser,adh,fin}$ (blue shade curves) according to CEN/TS 19103 (2021) for different theoretical adhesive creep factors $\phi_{adh} = 0.6 - 5.0$. Red curve: Suggested curve from CEN/TS 19103 (2021) for $k'_{def} = 2k_{def} = 2 \cdot 0.6 = 1.2$. The example situation considers $\psi_{conn} = 1$, a continuous bondline, the timber section as reference, a span of $L = 5$ m, a concrete cross-section strip of h x b = 80 mm x 320 mm, and a concrete of class C30/37). See Fig. A.1 for a translation from γ to $EI_{ef}/EI_{\gamma=1}$.

3 Ultimate and serviceability limit state design

3.1 ULS bondline verification

3.1.1 Simple stress verification criteria

For design, the resulting and acting stress states on the ATCC element closely follow and result from the adhesive bondline properties (i.e. $K_{ser,adh}$ and γ) described above. For ATCC, experience shows that failures in beams designed for typical ULS and SLS situations may not be excluded to occur at the bondline itself, or more commonly, close to the bondline, e.g. in the form of cohesive failure of concrete (e.g. *Grönquist* et al. (2022)). As

a consequence, a verification of the adhesive bondline can be advised, especially in cases when the cross-section (height of timber and concrete) is chosen such that high shear stresses fall into the region of the bondline. This should consider the strength parameters of the adhesive, e.g. the shear strength of the bondline $f_{v,a}$ (see Subsection 2.1), and that of the substrates. Whether the bondlines are continuous or discontinuous, a simple stress verification condition for the ULS could be formulated as follows:

$$\tau_{v,Ed} \leq f_{v,Rd} = \min(f_{v,a,d}, f_{v,t,d}, f_{v,c,d}), \tag{8}$$

where $\tau_{v,Ed}$ is the acting design shear stress at the bondline, $f_{v,a,d}$ is the adhesive bondline design shear strength, $f_{v,t,d}$ is the design shear strength of the timber at the bondline, and $f_{v,c,d}$ is the design shear strength of the concrete at the bondline. For concrete, in particular, failing in a brittle manner, a shear strength $f_{v,c}$ is in theory non-existent as a parameter on its own, but rather a function of the concrete tensile strength. In fact, *Seim* & *Frohnmüller* (2022) propose to assume the concrete shear strength as twice the value of the surface tensile strength: $f_{\mathrm{v,c}} = 2 \cdot f_{\mathrm{ct,surf}}$.

Furthermore, and according to the current recommendation of CEN/TS 19103, 2021, tensile stresses perpendicular to the bondline σ_t shall be taken into account in design as 10% of the shear force. However, in the case of ATCC, a theoretical separation due to potential slab edge clamping effects (see e.g. *Schänzlin* & *Ramirez* (2020)), resulting in a loss of connection, as is e.g. the case with notches, might be practically ruled out due to the nature of an adhesive bondline (i.e. a force-based connection, no geometrical interlocking). However, the current state of knowledge on ATCC is still to sparse for entirely excluding σ_{t}, or assessing its effect on load-bearing capacity. *Kästner* & *Rautenstrauch* (2021) recommend to still consider σ_{t}, although no specific proposal is made. Therefore, for the perpendicular tensile stresses at the bondline, the following condition could potentially be applied:

$$\sigma_{t,Ed} \leq f_{t,Rd} = \min(f_{t,a,d}, f_{t,90,d}, f_{ct,surf,d}). \tag{9}$$

Hereby, $\sigma_{t,Ed}$ is the acting design stress perpendicular to the bondline, $f_{t,a,d}$ is the design tensile strength of the adhesive, and $f_{t,90,d}$ is the design tensile strength of the timber perpendicular to the grain direction. Even though further research and insight is necessary, the simple conditions of Eq. 8 and Eq. 9 would represent first possible (but not necessarily conservative, see Section 3.1.2) steps towards the formulation of design criteria at adhesive bondlines of ATCC.

3.1.2 Complex stress states and failure criteria

While simplified design methods as presented in the sections above might be sufficient for most practical cases, it may be interesting to consider multiple arising stress components at the bondline in a combined failure criteria in case of special situations. These stress

components, for a specified location along the span, might be a mix of the (main) longitudinal shear stresses, the tensile stresses perpendicular to the bondline, and also possible stresses in transverse direction (biaxial effects). Conveniently, the occurring stress states and possible failure criteria would be investigated using more complex modelling, e.g. using Finite Element models (e.g. *Zauft* (2014), *Eisenhut* & *Seim* (2016), *Tannert* et al. (2017), Hampel (2021)).

3.2 Long-term ULS bondline verification and SLS design at $t \neq 0$

In addition to the short term stresses described above, long-term stresses in the members and on the bondline develop due to "inelastic" effects such as creep and shrinkage of concrete, creep and swelling/shrinkage of timber, and temperature differences, as well as due to the effect of these happening differently in timber and concrete, and on different magnitudes at different time scales. CEN/TS 19103 (2021) states that for each relevant time state, these inelastic influences shall be considered for both the ULS and the SLS. Furthermore, annex B of CEN/TS 19103 (2021) provides a method for the analytical estimation of these effects in conjunction with the γ-method for metallic fasteners and notches. From literature, it is well known that stresses as well as deformations due to a differential strain $\Delta\varepsilon$ (i.e. the inelastic effects described above) in two members of a bonded composite (a "bilayer") maximize when the bondline is rigid (see e.g. *Timoshenko* (1925) or *Grönquist* (2020)). This aspect is to a priori already considered in CEN/TS 19103 (2021) with an equivalent "fictitious load" p_{sls}:

$$p_{sls} = \frac{\pi^2 E_1 A_1 E_2 A_2 z \gamma \Delta\varepsilon}{(E_1 A_1 + E_2 A_2) L^2}. \tag{10}$$

Hereby E_1 and E_2 are the elastic moduli of the layers (denoted 1 and 2, e.g. concrete and timber), $A_1 = h_1 b_1$ and $A_2 = h_2 b_2$ are the cross-sectional areas of the layers, with h_1 and h_2 being the layer heights (or thicknesses), and $z = (h_1 + h_2)/2$ is the distance of centroids ($z = (h_1 + h_2)/2 + h_{adh}$ in the case of an adhesive bondline of thickness h_{adh}), and L is the span. From Eq. 10, it can be seen that p_{sls} is maximized when $\gamma = 1$. This equivalent "fictitious load" has to be considered for ULS and SLS design. Furthermore, for $\gamma \leq 1$, the effective flexural rigidity EI_{ef} is additionally to be reduced by a factor $C_{J,sls}$. However, $C_{J,sls} = 1$ in the case of a rigid adhesive bondline. It remains to be investigated, if the factors p_{sls} and $C_{J,sls}$ are indeed well calibrated with respect to their applicability to adhesive bondlines. In the case of a continuous and fully rigid bondline, according to *Timoshenko* (1925), the curvature χ_{inel} due to the differential (or difference of inelastic) strain $\Delta\varepsilon$ is formulated as follows:

$$\chi_{inel} = \frac{\Delta\varepsilon}{z + \frac{2(E_1 h_1^3/12 + E_2 h_2^3/12)}{h_1 + h_2} \left(\frac{1}{E_1 h_1} + \frac{1}{E_2 h_2} \right)}. \tag{11}$$

In the case of a simply supported beam, the theoretical and equivalent load necessary in order to result in a beam curvature of χ_{inel} can be expressed as:

$$q_{eqiv,inel} = \frac{8(EI_{ef})}{L^2} \cdot \chi_{inel}, \tag{12}$$

where (EI_{ef}) is the effective flexural rigidity in the case of a rigid bondline ($\gamma = 1$), e.g. in the case where the reference axis is chosen in material 2 (EI_{ef}) is expressed as:

$$(EI_{ef}) = E_2 \left(n_1 I_1 + I_2 + \gamma n_1 A_1 \frac{A_2 z^2}{\gamma n_1 A_1 + A_2} \right). \tag{13}$$

Hereby, $I_1 = h_1^3 b_1/12$ and $I_2 = h_2^3 b_2/12$ are the second area moments of inertia, and $n_1 = E_2/E_1$. Preliminary calculations indicate that, e.g. when comparing Eq. 12 with Eq. 10 for the case of the ATCC setup from Fig. A.1, the fictitious load p_{sls} results in a 23% higher value than compared to $q_{eqiv,inel}$, meaning that the use of p_{sls} might be overly conservative. Whether this can be generalized to any arbitrary ATCC situation of fully rigid and continuous bondlines remains to be investigated. However, preliminary calculations using more complex rheological material models in conjunction with the Finite Element Method show that the method of annex B of CEN/TS 19103 (2021) is in most cases conservative for ATCC elements, at least with respect to SLS deformations (Hampel (2021)). And the analytical derivations of the factors from CEN/TS 19103 (2021) in *Schänzlin* (2003) do not necessarily exclude the case of adhesive bondlines. However, they were derived under the assumption of sinusoidal-distributed inelastic strains, instead of the simpler but more realistic case of constant inelastic strains along the length as in *Timoshenko* (1925).

Regarding long-term ULS bondline verification, investigations using numerical modelling have been made by *Eisenhut* & *Seim* (2016), where long-term stress development has been analyzed, or by *Erlinger* et al. (2020). In the case of ATCC, such complex models can generally be recommended over the simplified procedure of annex B of CEN/TS 19103 (2021). This is especially the case for discontinuous or flexible bondlines, or in general, for situations where the γ-method might be limited (*Huber* & *Deix* (2021)).

4 Conclusions and outlook

From the parametric studies in Section 2, it could be seen that the specific ATCC execution types (see Tab. 1) can have a large influence on bondline properties required for design. It was shown that for most cases of rigid and continuous bondlines $\gamma \approx 1$, and that the determination of a bondline slip modulus $K_{ser,adh}$ is not necessary. However, it was also shown that this is not always the case for flexible interlayers (e.g. soft adhesives) or for discontinuous bondlines. Here, it can be advised to experimentally determine a value of $K_{ser,adh}$, since in some cases $\gamma < 1$ may result.

Concerning ULS and SLS design, where stresses and deformations directly result from the aforementioned bondline properties, simple and preliminary design conditions can be formulated for the adhesive bondline, e.g. as in Eq. 8 and Eq. 9. However, here, further research and investigation is necessary; conveniently, using adequate Finite Element models along experimental validation. However, since instead of bondline properties, rather inelastic effects (creep and shrinkage/swelling of concrete and timber) are governing the long-term behavior, it can be advised to focus on reliable modelling of not only the adhesive bondline, but specifically on that of the timber and the concrete, with respect to different execution types (e.g. dry or wet processes). In fact, for TCC elements, regardless of the connection system, the deformations in SLS design are often decisive (*Müller* et al. (2021)). This aspect is critical for ATTC, since here, a trade-off between composite efficiency and maximum effect of inelastic strains is made.

Further aspects, e.g. regarding execution, behavior in the fire situation, or the important aspect of bondline durability assessment (relevant work is given e.g. in *Loulou* (2013), *Frohnmüller* et al. (2021), *Frohnmüller*; *Wisner*, et al. (2022), and *Frohnmüller*; *Ho*, et al. (2022)), directly influence and may play a major role with respect to the design procedure. However, these aspects remain to be investigated conclusively, and highly depend on the used product combination, such that they may better be considered e.g. in the frame of European technical assessments (ETA's), respectively. Nevertheless, since ATCC are not yet included in standardization due to their relative novelty, but that it is to be expected that ATCC will be of imminent practical relevance, we recommend, besides pursuing on-going research efforts, to initiate a working group for including ATCC-specific considerations in view of harmonized standardization for structural design.

5 Acknowledgements

We sincerely thank Jens Frohnmüller and Werner Seim for their invaluable contribution to this paper, as well as Jörg Schänzlin and Gerhard Dill-Langer for discussion. Furthermore, we would like to express our gratitude to the INTER members for the valuable feedback received during the INTER 2023 meeting. This paper has been initiated within the Working Group 4 of COST Action CA20139 "Holistic design of taller timber buildings – HELEN".

6 References

Arendt, S.; M. Sutter; M. Breidenbach; R. Schlag & V. Schmid (2022). "Neue Forschungsergebnisse zu Nass-in-Nass geklebten Holz-Beton-Verbunddecken." In: *Bautechnik* 99. DOI: 10.1002/bate.202200068.

Bajzecerová, V.; J. Kanócz; M. Rovňák & M. Kováč (2022). "Prestressed CLT-concrete composite panels with adhesive shear connection." In: *Journal of Building Engineering* 56, p. 104785. ISSN: 2352-7102. DOI: 10.1016/j.jobe.2022.104785.

Binder, E.; W. Derkowski & T. Bader (2023). *Short-term creep tests for shear connections of timber-concrete-comosite slabs*. Proceedings ICEM20- 20th International Conference on Experimental Mechanics Porto 2-7 July 2023.

CEN/TS 19103 (2021). *Eurocode 5: Design of Timber Structures – Structural design of timber-concrete composite structures – Common rules and rules for buildings*. European Committee for Standardization (CEN): Brussels, Belgium, 2021.

Dias, A.; J. Schänzlin & P. Dietsch (2018). *Design of timber-concrete composite structures: A state-of-the-art report by COST Action FP1402 WG 4*. Tech. rep. Shaker Verlag, Aachen.

Dias, A. M. P. G. (2005). "Mechanical behaviour of timber-concrete joints." PhD thesis. TU Delft, Faculty Of Civil Engineering and Geosciences, ISBN 90-901-9214-X.

DIN EN 1995-1-1/NA (2013). *Nationaler Anhang – Eurocode 5: Bemessung und Konstruktion von Holzbauten – Teil 1-1: Allgemeines – Allgemeine Regeln und Regeln für den Hochbau*. DIN Deutsches Institut für Normung e. V., Berlin.

Eisenhut, L. & W. Seim (2016). "Langzeitverhalten geklebter Bauteile aus Holz und hochfestem Beton bei natürlichem Klima." In: *Bautechnik* 93.11, pp. 807–816. DOI: 10.1002/bate.201500087.

EN 14358 (2016). *Timber structures – Calculation and verification of characteristic values*. European Committee for Standardization (CEN): Brussels, Belgium, 2016.

EN 1992-1-1 (2004). *Eurocode 2: Design of concrete structures—Part 1-1: General rules and rules for buildings*. European Committee for Standardization (CEN): Brussels, Belgium, 2004; with corrections and amendments + AC:2010, A1:2014.

EN 1995-1-1 (2004). *Eurocode 5: Design of timber structures — Part 1-1: General rules and rules for buildings*. European Committee for Standardization (CEN), Brussels, Belgium, with corrections and amendments + AC:2006 and A1:2008.

Erlinger, G.; C. Hackspiel & K. Nachbagauer (2020). "Rechenmodelle für geklebte Holz-Beton-Verbundkonstruktionen." In: *The journal of OIAV, Österreichische Ingenieur- und Architektenzeitschrift* 165.

Frohnmüller, J.; J. Fischer & W. Seim (2021). "Full-scale testing of adhesively bonded timber-concrete composite beams." In: *Materials and Structures* 54(187). DOI: 10.1617/s11527-021-01766-y.

Frohnmüller, J.; A. Ho & W. Seim (2022). *Versuche zum Nachweis der Dauerhaftigkeit der Verklebung - Zwischenbericht 07 des ZIM Projekts "Entwicklung einer Schnellbaumethode für HBV-Decken mittels Verklebung vorgefertigter Betonelemente" (ZF4147005EB9)*. Tech. rep. Universität Kassel, Fachgebiet Bauwerkserhaltung und Holzbau.

Frohnmüller, J.; W. Seim; C.Umbach & J. Hummel (2023). "Adhesively bonded timber-concrete composite construction method (ATCC)- pilot application in a school building in germany." In: *World Conference on Timber Engineering 2023 (WCTE2023)*. DOI: 10.52202/069179-0542.

Frohnmüller, J.; G. Wisner; T. Waschkowitz; M. Merono; C. Ueckermann; E. Stammen & K. Dilger (2022). "Durability of Adhesively Bonded Timber-Concrete-Composite Constructions Joined by Fast Heated Structural Adhesive Bond Lines." In: *Durability of Building and Construction Sealants and Adhesives: 7th Volume, ASTM International* 247, pp. 128–151. DOI: 10.1520/STP163320200063.

Fu, Q.; L. Yan & B. Kasal (2022). "Bending behavior of adhesively-bonded engineered wood-concrete composite decks." In: *Acta Polytechnica CTU Proceedings* 33, pp. 175–180. DOI: 10.14311/APP.2022.33.0175.

Füchslin, M.; P. Grönquist; S. Stucki; T. Mamie; S. Kelch; I. Burgert & A. Frangi (2023). "Push-out tests of wet-process adhesive-bonded beech timber-concrete and timber-polymer-concrete composite connections." In: *World Conference on Timber Engineering 2023 (WCTE2023)*. DOI: 10.52202/069179-0422.

Grönquist, P. (2020). "Smart manufacturing of curved mass timber components by self-shaping." PhD thesis. ETH Zurich, Institute for Building Materials, Diss. ETH No. 26610. DOI: 10.3929/ethz-b-000405617.

Grönquist, P.; M. Füchslin; S. Gianinazzi; A. Albertini; S. Stucki; I. Burgert; T. Mamié; S. Kelch & A. Frangi (2022). *Tragverhalten von verklebten Holz-Beton- und Holz-Polymerbeton-Verbunddecken mit Buchen-Stabschichtholz,* tech. rep. S-WIN Swiss Wood Innovation Network, Tagungsband: Von der Forschung zur Praxis: Sicher mit Holz. DOI: 10.3929/ethz-b-000616135.

Hackspiel, C. (2020). *Verklebung als Verbund für Holz-Beton-Deckensysteme*. 1. Holzbau Kongress Berlin DHK 2020.

Hampel, D. (2021). *Modellieren des Langzeitverhaltens von Holz-Beton-Verbundelementen mit Buchen-Stabschichtholz*. Master thesis, ETH Zurich, Institute of Structural Engineering. Available upon request to P. Grönquist, A. Frangi.

Huber, C. & K. Deix (2021). "Comparison of Calculation Methods of Elastic Bonding: Limits of the Gamma Method Using an Example of a Wood & Concrete Composite Floor with Single Loads." In: *Materials* 14.23. DOI: 10.3390/ma14237211.

Kästner, M. & K. Rautenstrauch (2021). "Polymermörtel-Klebverbindungen für Holz-Beton-Verbundbrücken Teil 1." In: *Bautechnik* 98. DOI: 10.1617/s11527-021-01766-y.

Kreuzinger, H. (2000). "Die Holz-Beton-Verbundbauweise." In: *HOLZ, Informationsdienst (Ed.): Fachtagung Holzbau 1999-2000, Holzbau für das neue Jahrhundert, 2000, pp. 70-83*.

Loulou, L. (2013). "Durabilité de l'assemblage mixte bois-béton collé sous chargement hydrique." PhD thesis. Université Paris Est, École doctorale Sciences, Ingénierie et Environnement (en partenariat avec Laboratoire Navier).

Michelfelder, B. (2006). "Trag- und Verformungsverhalten von Kerven bei Brettstapel-Beton-Verbunddecken." PhD thesis. Universität Stuttgart, Institut für Konstruktion und Entwurf, Nr. 2006-1, ISSN 1439-3751.

Müller, K. (2020). “Timber-concrete composite slabs with micro-notches.” PhD thesis. ETH Zurich, Institute of Structural Engineering, Diss. ETH No. 27083. DOI: 10.3929/ethz-b-000474874.

Müller, K.; P. Grönquist; A. S. Cao & A. Frangi (2021). “Self-camber of timber beams by swelling hardwood inlays for timber–concrete composite elements.” In: *Construction and Building Materials* 308, p. 125024. DOI: 10.1016/j.conbuildmat.2021.125024.

Schänzlin, J. (2003). “Zum Langzeitverhalten von Brettstapel-Beton-Verbunddecken.” PhD thesis. Universität Stuttgart, Institut für Konstruktion und Entwurf, Nr. 2003-2, ISSN 1439-3751.

Schänzlin, J. & S. Mönch (2017). “Push-out vs. beam: Can the results of experimental stiffness of TCC-connectors be transferred?” In: *Reinhard Brandner, Andreas Ringhofer and Philipp Dietsch (Hg.): International Conference on Connections in Timber Engineering - From Research to Standard. COST Action FP1402. Graz, 13.09.2017, pp. 122–134*.

Schänzlin, J. & C. Ramirez (2020). *Entwurf und Entwicklung von Details bei Holz-Beton Verbundbauteilen für den Einsatz im Hochbau (HIP 1165437)*. Tech. rep. Hochschule Biberach, Institut für Holzbau.

Seim, W. & J. Frohnmüller (2022). “Holz-Beton Verbund mit verklebten Fertigteilen – konsequenter Trockenbau.” In: *26. Internationales Holzbau-Forum IHF 2022*.

Śliwa-Wieczorek, K.; W. Derkowski; E. Binder; A. Kwiecień; B. Zając; E. Halilovic & S. Lotinac (2023). “Shear Stiffness and Capacity of PolyUrethane Flexible Joint in Timber-Concrete Composites.” In: *Building for the Future: Durable, Sustainable, Resilient*. Ed. by A. Ilki; D. Çavunt & Y. S. Çavunt. Cham: Springer Nature Switzerland, pp. 476–485. DOI: 10.1007/978-3-031-32519-9_46.

Tannert, T.; B. Endacott; M. Brunner & T. Vallee (2017). “Long-term performance of adhesively bonded timber-concrete composites.” In: *International Journal of Adhesion and Adhesives* 72, pp. 51–61. DOI: 10.1016/j.ijadhadh.2016.10.005.

Tannert, T.; A. Gerber & T. Vallee (2020). “Hybrid adhesively bonded timber-concrete composite floors.” In: *International Journal of Adhesion and Adhesives* 97. DOI: 10.1016/j.ijadhadh.2019.102490.

Timoshenko, S. (1925). “Analysis of bi-metal thermostats.” In: *Journal of the Optical Society of America* 11.3, p. 233–255. DOI: 10.1364/JOSA.11.000233.

Töpler, J.; M. Schweigler; R. Lemaître; P. Palma; M. Schenk; P. Grönquist; C. Tapia; G. Hochreiner & U. Kuhlmann (2023). “Finite element based design of timber structures.” In: *Proceedings of the 10th meeting of INTER, International Network on Timber Engineering Research*.

Zauft, D. (2014). “Untersuchungen an geklebten Verbundkonstruktionen aus Holz und Leichtbeton.” PhD thesis. Technische Universität Berlin. ISBN: 978-3-8440-3200-0.

A Appendix: γ vs. $EI_{ef}/EI_{\gamma=1}$

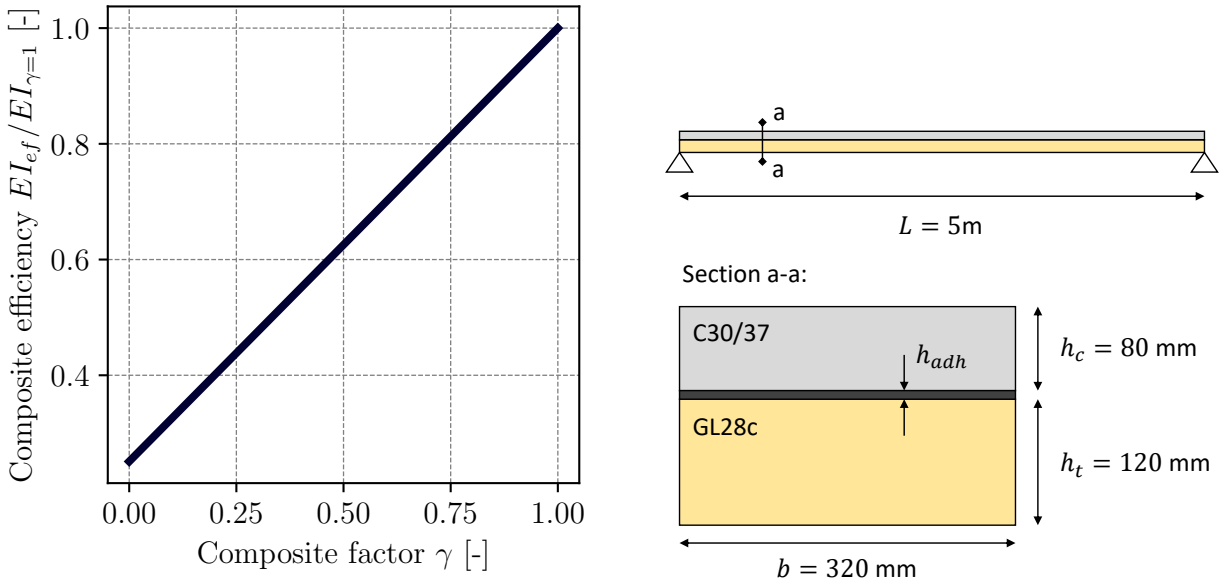

Figure A.1. ***Left****: Composite efficiency $EI_{ef}/EI_{\gamma=1}$ as a function of composite factor γ. Translation in the case of the shown γ-values of the parametric studies in this paper.* ***Right****: The example situation considers the timber section as reference, a span of L = 5 m, a timber cross-section of h x b = 120 mm x 320 mm, a timber of class GL28c, a concrete cross-section of h x b = 80 mm x 320 mm, and a concrete of class C30/37. EI_{ef} is calculated using Eq. 13.*